JAIST Repository
https://dspace.jaist.ac.jp/

Title	Low-frequency noise in InAs films bonded on low-k flexible substrates
Author(s)	Le, Son Phuong; Ui, Toshimasa; Suzuki, Toshi-kazu
Citation	Applied Physics Letters, 107(19): 192103-1-192103-4
Issue Date	2015-11-09
Type	Journal Article
Text version	publisher
URL	http://hdl.handle.net/10119/15422
Rights	Copyright 2015 American Institute of Physics. This article may be downloaded for personal use only. Any other use requires prior permission of the author and the American Institute of Physics. The following article appeared in Son Phuong Le, Toshimasa Ui, and Toshi-kazu Suzuki, Applied Physics Letters, 107(19), 192103 (2015) and may be found at http://dx.doi.org/10.1063/1.4935458
Description	

Japan Advanced Institute of Science and Technology

Low-frequency noise in InAs films bonded on low-*k* flexible substrates

Son Phuong Le, Toshimasa Ui, and Toshi-kazu Suzuki[a)]
Center for Nano Materials and Technology, Japan Advanced Institute of Science and Technology (JAIST), 1-1 Asahidai, Nomi, Ishikawa 923-1292, Japan

(Received 30 August 2015; accepted 27 October 2015; published online 9 November 2015)

We have systematically investigated low-frequency noise (LFN) in InAs films with several thicknesses ($\simeq$ 10-100 nm) bonded on low-*k* flexible substrates (InAs/FS), comparing with that in InAs films epitaxially grown on GaAs(001) substrates (InAs/GaAs). We obtain current LFN spectra exhibiting approximate $1/f$ characteristics and consequent effective Hooge parameters α depending on the thickness, where we find that α in the InAs/FS is larger than that in the InAs/GaAs. The behavior of α can be attributed to the fluctuation of the electron mobility dominated by surface/interface charge scattering and by thickness fluctuation scattering. © *2015 AIP Publishing LLC.*
[http://dx.doi.org/10.1063/1.4935458]

A narrow-gap compound semiconductor InAs has attractive properties,[1,2] applicable to mid-infrared optical devices,[3] ultra-high-speed electron devices,[4–6] and also interband tunnel devices.[7,8] Moreover, heterogeneous integration of InAs film devices on host substrates was realized with excellent device performances.[9–11] Previously, we fabricated InAs films bonded on host low-dielectric-constant (low-*k*) flexible substrates (FS),[12–14] by using epitaxial lift-off (ELO) and van der Waals bonding (VWB) method,[15,16] investigating electron scattering and carrier recombinations in the InAs films. As a result, we found important roles of surface/interface charge scattering and thickness fluctuation scattering in the InAs films bonded on low-*k* FS.[13] Such specific scattering mechanisms might be responsible for electronic noise characteristics through fluctuations of both the electron number and the mobility in the InAs films, especially for low-frequency noise (LFN) according to slow dynamics of trapping/detrapping of surface/interface charges. Even though the DC electronic properties are elucidated, the LFN in the InAs films bonded on low-*k* FS remains an issue. Although there were several studies on LFN in InAs devices based on the 6.1 Å family heterostructures,[17–21] InAs devices on host substrates are different in the formation method and also in the electron scattering mechanisms. Moreover, it was often difficult to elucidate the underlying mechanisms behind the LFN. In this work, we carried out a systematic investigation on LFN in the InAs films bonded on low-*k* FS (InAs/FS) with the film thicknesses $d \simeq$ 10-100 nm, comparing with that in InAs films epitaxially grown on GaAs(001) substrate (InAs/GaAs); this can illustrate insights into InAs devices on host substrates.

Using the InAs(thickness $\simeq$ 500 nm)/FS and the InAs(thickness $\simeq$ 500 nm)/GaAs, Hall-bars and two-terminal (2T) devices were fabricated. The fabrication process is the same as the previous report;[12,13] we employed the ELO and "inverted" VWB process shown in Fig. 1 for the InAs/FS, in which the InAs device layer was "inverted" and bonded onto a host low-*k* FS, polyethylene terephthalate coated by bisazide-rubber. To obtain several InAs film channel thicknesses $d \simeq$ 10-100 nm, the recess thinning process was carried out, where the "inverted" VWB process is advantageous to obtain a high crystal quality after the recess thinning according to the growth-direction dislocation distribution.[22] The top InAs surfaces for both the InAs/FS and the InAs/GaAs are not covered by anything. The 2T devices have InAs channel width W = 20-100 μm and length L = 5-400 μm.

From Hall-bar measurements at room temperature, we obtain the electron mobility μ and the sheet electron concentration n_s as functions of the InAs film thickness d, as shown in Fig. 2, where the error bars come from the thickness measurements by laser scanning microscope as described in Ref. 13. Although n_s exhibits a variation, μ shows systematic behaviors well-fitted by $1/\mu = 1/\mu_0 + 1/\mu_C + 1/\mu_{TF}$, where μ_0 is a thickness-independent constant mobility, μ_C is a mobility due to Coulomb scattering by surface/interface charges, and μ_{TF} is a mobility due to thickness fluctuation scattering, each given by the following.[13] The thickness-independent constant mobility is $\mu_0 \simeq 14\,000\,\mathrm{cm^2/V\text{-}s}$, owing to polar optical phonon scattering giving a mobility of $\mu_{ph} \simeq 25\,000\,\mathrm{cm^2/V\text{-}s}$[23] and to possible additional scattering independent of the thickness. The surface/interface charge scattering mobility[24–26] and the thickness fluctuation scattering mobility[25–30] are given by

$$\mu_C = \frac{4\pi\varepsilon_s{}^2\hbar^3 k_F{}^3}{n_c e^3 m^{*2}} d = Ad \quad \text{and} \quad \mu_{TF} = Bd^{\gamma}\ (\gamma \simeq 5.2), \quad (1)$$

respectively, with constants A and B, the surface/interface charge density n_c, which is the sum of the charge density at the surface and the InAs-FS or InAs-GaAs interface, the dielectric constant ε_s, the electron effective mass m^*, and the Fermi wave vector k_F. The fitting gives $n_c \sim 1 \times 10^{12}\,\mathrm{cm^{-2}}$ (InAs/FS) and $\sim 9 \times 10^{13}\,\mathrm{cm^{-2}}$ (InAs/GaAs), and we obtain $\gamma \simeq 5.2$ experimentally and numerically.[13] The obtained n_c for the InAs/GaAs is quite larger than that for the InAs/FS, indicating the dominance of the InAs-GaAs interface in comparison with the surface. For the InAs/FS, since the thickness fluctuation scattering is dominant in the regime of $d \lesssim 15$ nm, we can obtain the value of B by fitting, while we cannot for the InAs/GaAs, which does not show such regime

a)Author to whom correspondence should be addressed. Electronic mail: tosikazu@jaist.ac.jp

 © 2015 AIP Publishing LLC

This article is copyrighted as indicated in the article. Reuse of AIP content is subject to the terms at: http://scitation.aip.org/termsconditions. Downloaded to IP: 221.133.114.20 On: Mon, 09 Nov 2015 15:20:06

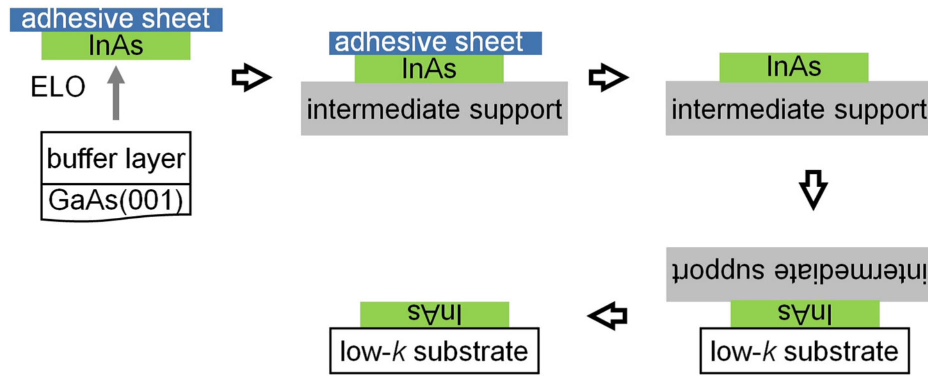

FIG. 1. Schematic of the formation of InAs films on low-k flexible substrates. The InAs device layer is "inverted" and bonded.

because of low surface/interface charge scattering mobilities. However, the InAs/FS exhibits a smaller B than the InAs/GaAs, indicating a larger thickness fluctuation (maybe short-range one relevant to quantum scattering).

We carried out LFN characterization of the 2T devices, which show Ohmic I-V characteristics, by using the same measurement system as Ref. 31. Figures 3(a) and 3(b) show examples of measurement results of current noise power spectrum density S_I for the Ohmic regime of the InAs/FS and the InAs/GaAs devices, respectively, with the InAs film thickness $d \simeq 10$, 30, 100 nm, $W = 50\,\mu$m, $L = 350\,\mu$m (InAs/FS), and $L = 400\,\mu$m (InAs/GaAs). We obtain approximate $1/f$ spectra satisfying $S_I/I^2 \simeq K/f^{\beta}$, with $\beta \sim 1$ and a constant factor K, where the DC current I is varied by changing the noiseless 2T bias voltage V. As shown in the insets of Figs. 3(a) and 3(b), plotting $S_I f$ at $f = 1$ Hz as a function of I, where $S_I f \propto I^2$ is confirmed, we evaluate the factor $K = S_I f/I^2$. In order to check the channel size (width and length) dependence of K, in Fig. 4, we plot the factor K as a function of the total electron number in the InAs channel $N = LWn_s$. We obtain the relation $K \propto 1/N$, indicating the LFN dominated by the InAs channel with a negligible contribution from the contact and electrode. The effective Hooge parameters[32] $\alpha = S_I fN/I^2 = KN$, obtained by fitting of K as a function of N, are shown in Fig. 5(a) as a function of the InAs film thickness d. We observe that α in the InAs/FS is larger than that in the InAs/GaAs. Figures 5(b) and 5(c) show α as the functions of μ and n_s, respectively. The Hooge parameters α are negatively correlated with μ as well as d, whereas uncorrelated with n_s, suggesting that the mobility fluctuation is more important.

We consider $\alpha = \alpha_\mu + \alpha_N \sim (\delta\mu)^2/\mu^2 + (\delta N)^2/N$ based on the Burgess theorem,[31–36] where $\delta\mu$ and δN are the fluctuations of the mobility μ and the electron number N relevant to $1/f$ noise, respectively. If the electron number fluctuation is dominant, $\alpha \simeq \alpha_N \sim (\delta N)^2/N$. The electron number fluctuation caused by trapping/detrapping at the surface/interface states with a density D_i gives $\alpha \sim D_i k_B T/n_s \propto 1/n_s$,[37] which is not the case as in Fig. 5(c). We hence consider that the mobility fluctuation is dominant, $\alpha \simeq \alpha_\mu \sim (\delta\mu)^2/\mu^2$, where

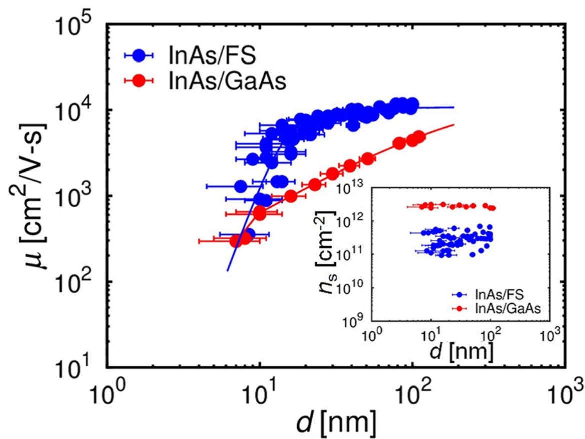

FIG. 2. The electron mobility μ as a function of the InAs film thickness d with fitting curves. The inset shows the sheet electron concentration n_s as a function of d.

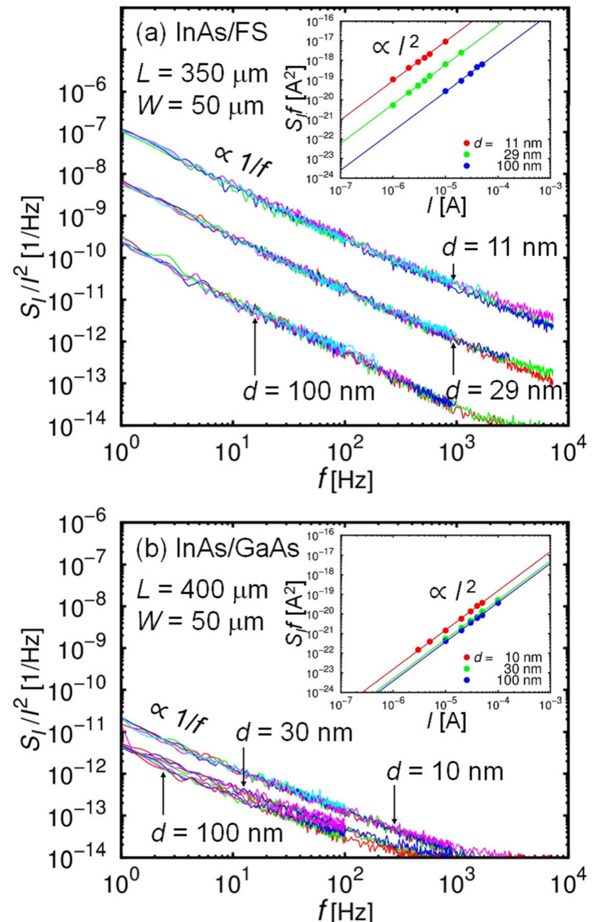

FIG. 3. S_I/I^2 as a function of f for (a) InAs/FS and (b) InAs/GaAs. The insets show $S_I f$ at 1 Hz as a function of I, confirming $S_I f \propto I^2$.

This article is copyrighted as indicated in the article. Reuse of AIP content is subject to the terms at: http://scitation.aip.org/termsconditions. Downloaded to IP: 221.133.114.20 On: Mon, 09 Nov 2015 15:20:06

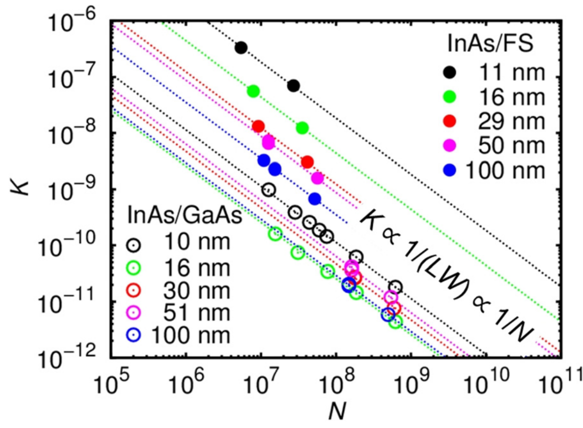

FIG. 4. The factor K as a function of the total electron number N, exhibiting $K \propto 1/N$.

$$\frac{\delta\mu}{\mu^2} \simeq \frac{\delta\mu_0}{{\mu_0}^2} + \frac{\delta\mu_C}{{\mu_C}^2} + \frac{\delta\mu_{TF}}{{\mu_{TF}}^2} \tag{2}$$

with obvious notations. We consider that the fluctuations of $\mu_C \propto d/n_c$ and $\mu_{TF} \propto d^\gamma$ are related to spatial randomness[38,39] based on the following picture. The surface/interface charges are distributed randomly and fluctuate slowly, making a time-dependent random potential with slow dynamics. In addition, while the InAs film thickness d means the spatially averaged one, there is a spatial thickness inhomogeneity (fluctuation), making a random potential through the spatial fluctuation of quantum levels. The surface/interface charges and the spatial thickness fluctuation uncorrelatedly make a slowly time-dependent total random potential.

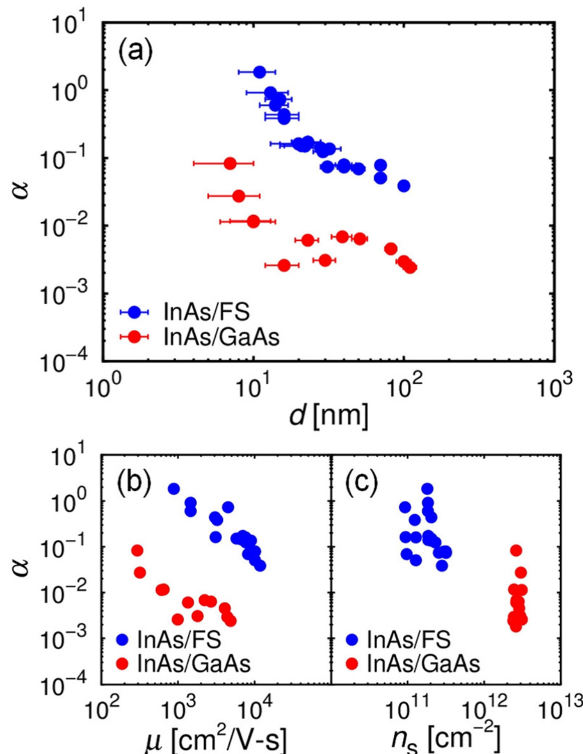

FIG. 5. The Hooge parameter α as the functions of (a) the InAs film thickness d, (b) the electron mobility μ, and (c) the electron sheet concentration n_s.

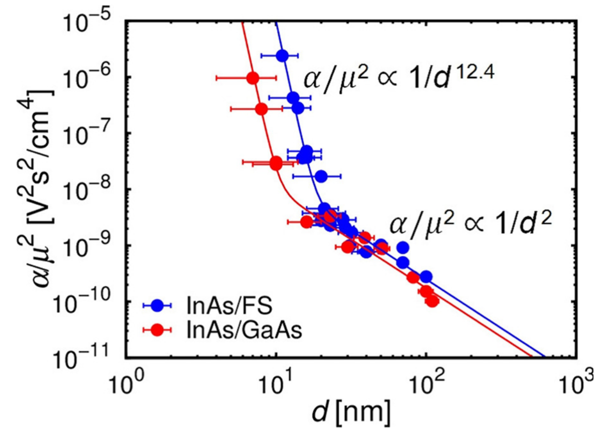

FIG. 6. α/μ^2 as a function of the InAs film thickness d.

Under the time-dependent random potential, an electron wave function tends to be localized, whose position slowly fluctuates, leading to a slow fluctuation of the film thickness at the electron position. Therefore, the temporal fluctuation of $\mu_C \propto d/n_c$ and $\mu_{TF} \propto d^\gamma$ will reflect the spatial fluctuation δd (maybe long-range one). Also, while n_c is the spatially averaged surface/interface charge density, there is a spatial density inhomogeneity (fluctuation). Thus, the slow fluctuation of the electron position leads to a slow fluctuation of the surface/interface charge density at the electron position. Therefore, the spatial fluctuation δn_c will induce the temporal fluctuation of $\mu_C \propto d/n_c$. According to the picture, we assume the order of the fluctuations $\delta\mu_C/\mu_C \sim (\delta d/d - \delta n_c/n_c)$ and $\delta\mu_{TF}/\mu_{TF} \sim \gamma\delta d/d$, leading to

$$\begin{aligned}\frac{\delta\mu}{\mu^2} &\sim \frac{\delta\mu_0}{{\mu_0}^2} + \frac{1}{\mu_C}\left(\frac{\delta d}{d} - \frac{\delta n_c}{n_c}\right) + \frac{\gamma}{\mu_{TF}}\frac{\delta d}{d} \\ &= \frac{\delta\mu_0}{{\mu_0}^2} + \left(\frac{1}{Ad} + \frac{\gamma}{Bd^\gamma}\right)\frac{\delta d}{d} - \frac{1}{Ad}\frac{\delta n_c}{n_c}\end{aligned} \tag{3}$$

using $\mu_C = Ad$ and $\mu_{TF} = Bd^\gamma$. As a result, we obtain

$$\frac{(\delta\mu)^2}{\mu^4} \sim \frac{\alpha}{\mu^2} \sim \frac{(\delta\mu_0)^2}{{\mu_0}^4} + \left(\frac{1}{Ad} + \frac{\gamma}{Bd^\gamma}\right)^2 \frac{(\delta d)^2}{d^2} + \frac{1}{A^2d^2}\frac{(\delta n_c)^2}{{n_c}^2} \tag{4}$$

similarly to Ref. 40. The first term including the polar optical phonon scattering mobility μ_{ph} should be independent of the thickness d and consequently is irrelevant to α depending on d. Moreover, if we assume the Hooge model,[32,35] it is plausible that the first term is negligible. Using the Hooge universal constant $\alpha_H \simeq 2 \times 10^{-3}$ (or less for low-dimensional InAs systems[41,42]), the contribution from the first term may be $\mu^2/{\mu_{ph}}^2 \times \alpha_H \ll 2 \times 10^{-3}$ and negligible in the measured $\alpha > 2 \times 10^{-3}$. Thus, by neglecting the first term of Eq. (4), we expect the relation

$$\frac{\alpha}{\mu^2} \sim \left[\frac{1}{A^2d^4} + \frac{2\gamma}{ABd^{(\gamma+3)}} + \frac{\gamma^2}{B^2d^{(2\gamma+2)}}\right](\delta d)^2 + \frac{(\delta n_c)^2}{A^2d^2{n_c}^2}. \tag{5}$$

In order to confirm this relation, measured α/μ^2 as a function of d is plotted in Fig. 6, with a fitting curve according to Eq. (5), where the fitting parameters are δn_c and δd (InAs/FS) or $\delta d^2/B^2$ (InAs/GaAs). We confirm that the measurement data

This article is copyrighted as indicated in the article. Reuse of AIP content is subject to the terms at: http://scitation.aip.org/termsconditions. Downloaded to IP: 221.133.114.20 On: Mon, 09 Nov 2015 15:20:06

TABLE I. The parameters of the InAs/FS and the InAs/GaAs.

	InAs/FS	InAs/GaAs
δd (nm)	~ 2	…
δn_c (cm^{-2})	$\sim 5 \times 10^{11}$	$\sim 4 \times 10^{12}$
n_c (cm^{-2})	$\sim 1 \times 10^{12}$	$\sim 9 \times 10^{13}$
$\sqrt{n_c}/\delta n_c$ (nm)	~ 20	~ 20

are well-fitted for both the InAs/FS and the InAs/GaAs. We find $\alpha/\mu^2 \propto 1/d^{(2\gamma+2)} \simeq 1/d^{12.4}$ dominated by the third term for small d, while $\alpha/\mu^2 \propto 1/d^2$ dominated by the fourth term for large d. It should be noted that $\delta\mu_{TF}$ giving the third term is important for $\delta\mu$, even though we do not observe μ dominated by μ_{TF} for the InAs/GaAs.

The fitting parameters and other parameters are summarized in Table I. We obtain a large $\delta d \sim 2$ nm for the InAs/FS, while δd for the InAs/GaAs cannot be estimated because we do not obtain the value of B. However, from the regime of $\alpha/\mu^2 \propto 1/d^{(2\gamma+2)}$, we find that $\delta d^2/B^2$ is larger for the InAs/FS than for the InAs/GaAs owing to the smaller B and/or larger δd, both meaning larger thickness fluctuations; the former may be short-range one, while the latter may be long-range one. Therefore, we consider that such larger thickness fluctuation is a reason of the fact that α in the InAs/FS is larger than that in the InAs/GaAs. This larger thickness fluctuation can be attributed to process inhomogeneity over the large channel area, owing to the relatively complicated fabrication process of the InAs/FS. On the other hand, we obtain $\delta n_c \sim 5 \times 10^{11}$ cm^{-2} (InAs/FS) and $\sim 4 \times 10^{12}$ cm^{-2} (InAs/GaAs), where the InAs/FS exhibits a quite smaller value. This can be attributed to the difference of n_c in the InAs/FS and the InAs/GaAs shown in Table I. If the surface/interface charges obey the Poisson distribution spatially, δn_c in the area S relevant to Coulomb scattering by the surface/interface charges satisfies $S^2 \delta n_c{}^2 \simeq S n_c$ and hence $\delta n_c \simeq \sqrt{n_c/S}$, suggesting that smaller δn_c is due to smaller n_c. In fact, we can estimate $\sqrt{S}$ by evaluating $\sqrt{n_c}/\delta n_c$ as shown in Table I, giving a common length of $\sqrt{S} \sim 20$ nm for both the InAs/FS and the InAs/GaAs. This should be a relevant length of Coulomb scattering by the surface/interface charges, which is similar to the Fermi wavelength, the two-dimensional screening length, or the phase coherence length.

In summary, we systematically investigated LFN in the InAs/FS, comparing with that in the InAs/GaAs. From the current LFN spectra exhibiting approximate $1/f$ characteristics, we obtained the effective Hooge parameters α depending on the InAs thickness, where we find that α in the InAs/FS is larger than that in the InAs/GaAs. The behavior of the Hooge parameters was analyzed and attributed to the fluctuation of the electron mobility dominated by surface/interface charge scattering and by thickness fluctuation scattering. The analysis gives an estimation of the thickness fluctuation, which is large for the InAs/FS, being a reason of the large Hooge parameter. Also, an estimation of the fluctuation of the surface/interface charge density is given, suggesting a relevant length of Coulomb scattering by the surface/interface charges.

This work was supported by JSPS KAKENHI Grant Nos. 26249046 and 15K13348.

[1] A. Milnes and A. Polyakov, Mater. Sci. Eng. B **18**, 237 (1993).
[2] H. Kroemer, Physica E **20**, 196 (2004).
[3] Z. Yin and X. Tang, Solid-State Electron. **51**, 6 (2007).
[4] B. R. Bennett, R. Magno, J. B. Boos, W. Kruppa, and M. G. Ancona, Solid-State Electron. **49**, 1875 (2005).
[5] D.-H. Kim and J. del Alamo, IEEE Electron Device Lett. **31**, 806 (2010).
[6] N. Li, E. S. Harmon, J. Hyland, D. B. Salzman, T. P. Ma, Y. Xuan, and P. D. Ye, Appl. Phys. Lett. **92**, 143507 (2008).
[7] Q. Zhang, W. Zhao, and A. Seabaugh, IEEE Electron Device Lett. **27**, 297 (2006).
[8] M. Luisier and G. Klimeck, IEEE Electron Device Lett. **30**, 602 (2009).
[9] H. Ko, K. Takei, R. Kapadia, S. Chuang, H. Fang, P. W. Leu, K. Ganapathi, E. Plis, H. S. Kim, S.-Y. Chen, M. Madsen, A. C. Ford, Y.-L. Chueh, S. Krishna, S. Salahuddin, and A. Javey, Nature **468**, 286 (2010).
[10] K. Takei, S. Chuang, H. Fang, R. Kapadia, C.-H. Liu, J. Nah, H. S. Kim, E. Plis, S. Krishna, Y.-L. Chueh, and A. Javey, Appl. Phys. Lett. **99**, 103507 (2011).
[11] K. Takei, H. Fang, S. B. Kumar, R. Kapadia, Q. Gao, M. Madsen, H. S. Kim, C.-H. Liu, Y.-L. Chueh, E. Plis, S. Krishna, H. A. Bechtel, J. Guo, and A. Javey, Nano Lett. **11**, 5008 (2011).
[12] H. Takita, N. Hashimoto, C. T. Nguyen, M. Kudo, M. Akabori, and T. Suzuki, Appl. Phys. Lett. **97**, 012102 (2010).
[13] C. T. Nguyen, H.-A. Shih, M. Akabori, and T. Suzuki, Appl. Phys. Lett. **100**, 232103 (2012).
[14] T. Suzuki, H. Takita, C. T. Nguyen, and K. Iiyama, AIP Adv. **2**, 042105 (2012).
[15] Y. Jeong, M. Shindo, M. Akabori, and T. Suzuki, Appl. Phys. Express **1**, 021201 (2008).
[16] Y. Jeong, M. Shindo, H. Takita, M. Akabori, and T. Suzuki, Phys. Status Solidi C **5**, 2787 (2008).
[17] M. Tacano, M. Ando, I. Shibasaki, S. Hashiguchi, J. Sikula, and T. Matsui, Microelectron. Reliab. **40**, 1921 (2000).
[18] W. Kruppa, J. Boos, B. Bennett, and M. Yang, Electron. Lett. **36**, 1888 (2000).
[19] W. Kruppa, M. J. Yang, B. R. Bennett, and J. B. Boos, Appl. Phys. Lett. **85**, 774 (2004).
[20] W. Kruppa, J. Boos, B. Bennett, and B. Tinkham, Solid-State Electron. **48**, 2079 (2004).
[21] W. Kruppa, J. Boos, B. Bennett, N. Papanicolaou, D. Park, and R. Bass, IEEE Trans. Electron Devices **54**, 1193 (2007).
[22] Y. Jeong, H. Choi, and T. Suzuki, J. Cryst. Growth **301–302**, 235 (2007).
[23] T. Suzuki, H. Ono, and S. Taniguchi, Sci. Technol. Adv. Mater. **6**, 400 (2005).
[24] T. H. Ning and C. T. Sah, Phys. Rev. B **6**, 4605 (1972).
[25] A. Gold, Solid State Commun. **60**, 531 (1986).
[26] A. Gold, Phys. Rev. B **35**, 723 (1987).
[27] H. Sakaki, T. Noda, K. Hirakawa, M. Tanaka, and T. Matsusue, Appl. Phys. Lett. **51**, 1934 (1987).
[28] C. R. Bolognesi, H. Kroemer, and J. H. English, Appl. Phys. Lett. **61**, 213 (1992).
[29] T. Ishihara, K. Uchida, J. Koga, and S. Takagi, Jpn. J. Appl. Phys., Part 1 **45**, 3125 (2006).
[30] A. Gold, J. Appl. Phys. **103**, 043718 (2008).
[31] S. P. Le, T. Q. Nguyen, H.-A. Shih, M. Kudo, and T. Suzuki, J. Appl. Phys. **116**, 054510 (2014).
[32] F. N. Hooge, IEEE Trans. Electron Devices **41**, 1926 (1994).
[33] R. E. Burgess, J. Phys. Chem. Solids **22**, 371 (1961).
[34] A. van der Ziel, Solid-State Electron. **17**, 110 (1974).
[35] F. N. Hooge, T. G. M. Kleinpenning, and L. K. J. Vandamme, Rep. Prog. Phys. **44**, 479 (1981).
[36] C. Surya and T. Y. Hsiang, Phys. Rev. B **35**, 6343 (1987).
[37] O. Jäntsch, IEEE Trans. Electron Devices **34**, 1100 (1987).
[38] O. Cohen, Z. Ovadyahu, and M. Rokni, Phys. Rev. Lett. **69**, 3555 (1992).
[39] O. Cohen and Z. Ovadyahu, Phys. Rev. B **50**, 10442 (1994).
[40] M. von Haartman, A. Lindgren, P.-E. Hellstrom, B. Gunnar Malm, S.-L. Zhang, and M. Ostling, IEEE Trans. Electron Devices **50**, 2513 (2003).
[41] M. R. Sakr and X. P. A. Gao, Appl. Phys. Lett. **93**, 203503 (2008).
[42] K.-M. Persson, B. G. Malm, and L.-E. Wernersson, Appl. Phys. Lett. **103**, 033508 (2013).

This article is copyrighted as indicated in the article. Reuse of AIP content is subject to the terms at: http://scitation.aip.org/termsconditions. Downloaded to IP: 221.133.114.20 On: Mon, 09 Nov 2015 15:20:06